

An Elastic-Plastic Constitutive Equation Taking Account of Particle Size and Its Application to A Homogenized Finite Element Analysis of A Composite Material

Shuji Takashima¹, Michihiko Nakagaki² and Noriyuki Miyazaki¹

Abstract: Composite materials have complicated microstructures. These microstructures affect the macroscopic deformation of composite materials. In the present study, we focus on the effect of particle size in a particle-dispersed composite material on the mechanical strength of the material. For this purpose, we derived a macroscopic elastic-plastic constitutive equation using a modified version of the Eshelby's equivalent inclusion method combined with the gradient plasticity. We incorporated this macroscopic elastic-plastic constitutive equation into a finite element program and performed a homogenized finite element analysis of a particle-dispersed composite material in which both the macroscopic and microscopic behaviors of the composite material were obtained. The present method successfully revealed the size effect in a particle-dispersed composite material, namely that its mechanical strength increases with a decrease in the particle size.

Keyword: size effect, composite material, Eshelby's theory, gradient plasticity.

1 Introduction

The microstructure of a polycrystalline material has a large effect on its macroscopic deformation behavior. In particular, the Hall-Petch effect is well known as a grain size miniaturization effect. Using this phenomenon, we can obtain high-strength materials by reducing the grain size. The mechanism of the Hall-Petch effect is explained as follows. Dislocations pile up at grain boundaries, with the grain boundaries resisting the dis-

location motion. When the grain size decreases, the ratio of the grain boundary volume to a unit volume of the material increases, hence the resistance to dislocation motion increases. Therefore, the material strength increases with a decrease in the grain boundary size. The same phenomenon occurs in particle-dispersed composite materials because hard particles included in the matrix material work to resist the dislocation motion. When the size of the hard particles decreases while a constant volume fraction of the particles is maintained, the strength of the composite material increases [Aikin and Christodoulou (1991), Lloyd (1994), Ling (2000)].

Standard plasticity theory cannot deal with the size effect on the strength of materials since it does not involve an internal length scale in the constitutive equation. There have been numerous studies dealing with this size effect on material strength. Among them, Liu and Hu (2005) predicted the particle size dependence of the overall plasticity for composite materials, using the micropolar theory. It seems difficult, however, to incorporate this theory into finite element programs, and a finite element analysis has not been carried out. Needleman (2000), and Yefimov, Groma, and Giessen (2004) performed finite element analyses of the size effect for composite materials using a crystal plasticity model with a discrete dislocation model. Very fine finite element models are employed in these analyses in order to account for the microstructure of composite materials.

Recently, much attention has been paid to higher-order gradient theories such as gradient dislocation dynamics, gradient plasticity, and gradient elasticity [Aifantis (2000)] because they can capture size effects. Among these, gradient plasticity

¹ Kyoto Univ., Sakyo-ku, Kyoto, Japan

² Kyushu Institute of Technology, Iizuka, Fukuoka, Japan

[Aifantis (2001)] successfully predicted the size effect on material strength. Zhu, Zbib, and Aifantis (1997) performed a size effect analysis of composite materials using gradient plasticity, but did not incorporate the theory into a finite element program. Nakagaki, Takashima, Matsumoto, and Miyazaki (2005) performed a finite element analysis that included the gradient plasticity, demonstrating the size effect on the strength of a particle dispersed composite material, as seen in Fig. 1 (b). The finite element model used in the analysis appears in Fig. 1 (a). Numerous finite elements are required in even the very simple structure depicted in Fig. 1 (a). In general, if an entire structure, including microstructure, is to be modeled using finite elements, an enormous number of such finite elements and an enormous amount of computational time will be required. To overcome these difficulties, various studies have been performed on the macroscopic constitutive equation for particle-dispersed composite materials in order to predict their mechanical behavior. Among these, the Eshelby's equivalent inclusion method [Eshelby (1957)] has been used for predicting the mechanical behavior of particle-dispersed composite materials. For example, Mori and Tanaka (1973) developed a mean field theory based on the Eshelby's equivalent inclusion method. They assumed that the stress and strain are uniform in each phase of a composite material and derived the elastic constitutive equation for composite materials. Tandon and Weng (1988) extended the Mori-Tanaka theory to an elastic-plastic constitutive equation for a particle-dispersed composite material.

In the present study, we focus on the particle size effect in particle-dispersed composite materials. For this purpose, we employ gradient plasticity [Zhu, Zbib, and Aifantis (1997)]. When we carry out finite element analyses of structures made of composite materials, the microstructures of the composite materials are often homogenized to reduce the total degree-of-freedom of the finite element model. Without such homogenization, it is practically impossible to apply gradient plasticity to a finite element stress analysis of structures made of composite materials. In the present study,

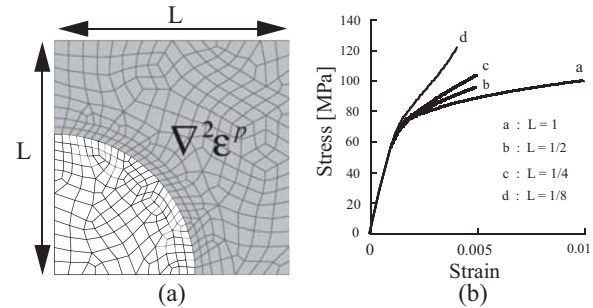


Figure 1: Previous study (a):Composite model with fine mesh (b):Macroscopic stress-strain curve for uniaxial tensile loading obtained from the gradient plasticity

we utilize the equivalent inclusion method for homogenization together with gradient plasticity to consider the particle size effect. In the Mori-Tanaka model and the Tandon-Weng model, the stress and strain distributions are not taken into account in deriving the elastic-plastic constitutive equation. We develop a new equivalent inclusion model to take account of both plastic strain in the matrix material and the strain distribution around particles. We then combine this equivalent inclusion model with the gradient plasticity to obtain a elastic-plastic constitutive equation that considers the size effect of particles in the microscopic region. We next incorporate the constitutive equation in a finite element program for homogenization. Finally, we will present the results of a numerical example for the size effect of particles on the strength of composite materials.

2 Equivalent inclusion method

We need a strain distribution in order to apply gradient plasticity, in which a strain gradient term is included. The equivalent inclusion method, as in the Mori-Tanaka model [Mori and Tanaka (1973)] and the Tandon and Weng model [Tandon and Weng (1988)], cannot be applied to gradient plasticity because they provide only the average strains in a matrix and an inclusion and do not provide the strain distribution in the matrix necessary for calculating the strain gradient term. In the present study, we derive the strains at arbitrary points in the matrix and the inclusion based

on the equivalent inclusion method, thus obtaining the strain distribution in the matrix.

2.1 Strain distribution at an arbitrary point

We assume that a single particle or an inclusion exists in a uniform infinite matrix. According to the Eshelby's equivalent inclusion method, we can evaluate the stresses and strains in the inclusion and the matrix under uniform loading, assuming that the real inclusion is replaced by a virtual inclusion or by an equivalent inclusion of the same material of the matrix with a specified eigenstrain. The total strain of the equivalent inclusion is given as follows:

$$\varepsilon_2 = \varepsilon_2^e + \varepsilon_2^* \quad (1)$$

where ε^* is the eigenstrain and subscripts 0, 1 and 2 indicate the respective quantities pertaining to the matrix at the infinite location, to the matrix, and to the inclusion. We assume that the composite material is subjected to a uniform strain ε_0 at the infinite location. Here we define the strain difference between ε_1 and ε_0 as ε_1^c , and that between ε_2 and ε_0 as ε_2^c .

$$\varepsilon_1(x) = \varepsilon_0 + \varepsilon_1^c(x), \quad \varepsilon_2 = \varepsilon_0 + \varepsilon_2^c \quad (2)$$

In Eq. 2, $\varepsilon_1(x)$ and $\varepsilon_1^c(x)$ indicate the functions of position, while ε_2 and ε_2^c in the inclusion are assumed to be constant. We can obtain $\varepsilon_1^c(x)$ and ε_2^c from the Eshelby's tensors ($S_{out}(x), S_{in}$) and the eigenstrain.

$$\varepsilon_1^c(x) = S_{out}(x) : \varepsilon^*, \quad \varepsilon_2^c = S_{in} : \varepsilon^* \quad (3)$$

The eigenstrain given by Eq. 3 is arbitrary. We consider the equivalent condition for the stress between the real inclusion and the equivalent inclusion and obtain the following equation.

$$\sigma_2 = \sigma_{eqv} = D_1^e : (\varepsilon_2 - \varepsilon^*), \quad \sigma_2 = D_2^e : \varepsilon_2 \quad (4)$$

Here, D_1^e and D_2^e are the elastic matrices for the matrix material and the inclusion. Using Eqs.2 to 4, we obtain the eigenstrain as a function of ε_0 that satisfies the equivalent condition.

$$\varepsilon^* = A_0 : \varepsilon_0 \quad (5)$$

$$A_0 = \left[(I \otimes I - (D_1^e)^{-1} : D_2^e)^{-1} - S_{in} \right]^{-1} \quad (6)$$

Here, I denotes the unit matrix. Substituting Eq. 5 into Eq. 3 and using Eq. 2, we can obtain the strains in the matrix and the inclusion, respectively as follows:

$$\varepsilon_1(x) = (I \otimes I + S_{out}(x) : A_0) : \varepsilon_0 \quad (7)$$

$$\varepsilon_2 = (I \otimes I + S_{in} : A_0) : \varepsilon_0 \quad (8)$$

As seen in Eqs. 7 and 8 the strains in both the matrix and the inclusion are calculated from the strain at the infinite location and from the several material properties included in D_1^e and D_2^e . The stresses in the matrix and the inclusion may then be written as

$$\sigma_1(x) = D_1^e : (I \otimes I + S_{out}(x) : A_0) : \varepsilon_0 \quad (9)$$

$$\sigma_2 = D_2^e : (I \otimes I + S_{in} : A_0) : \varepsilon_0 \quad (10)$$

2.2 Multi-particle model

We obtain the strain and stress distributions around a particle from Eqs.7 to 10. These distributions do not consider the interaction of particles, since the Eshelby's equivalent inclusion method assumes a single particle. Actually, many particles exist in the matrix. The interaction among particles creates more complicated stress and strain distributions. Here we consider such a situation.

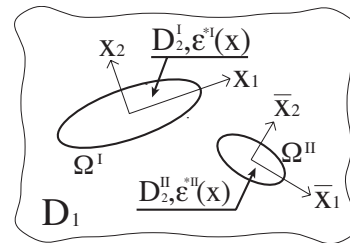


Figure 2: Multi-particle model.

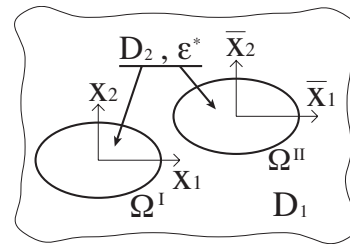


Figure 3: Simplification of multi-particle model.

Mura [Moschovidis and Mura (1975)] proposed an equivalent inclusion method for a multi-particle model. In the multi-particle case, the material, size, and direction of motion of the various particles may differ from particle to particle, as indicated in Fig. 2. Now let us consider the double-particle model in Fig. 2. The equivalent equations for particles Ω^I and Ω^{II} are given as follows:

$$D_2^I : (\varepsilon_0 + \varepsilon_2^c) = D_1 : (\varepsilon_0 + \varepsilon_2^c - \varepsilon^{*I}(x)) \quad \text{in } \Omega^I \quad (11)$$

$$D_2^{II} : (\varepsilon_0 + \varepsilon_2^c) = D_1 : (\varepsilon_0 + \varepsilon_2^c - \varepsilon^{*II}(\bar{x})) \quad \text{in } \Omega^{II} \quad (12)$$

where subscripts I and II indicate quantities pertaining to particles Ω^I and Ω^{II} , and the eigenstrains $\varepsilon^{*I}(x)$ and $\varepsilon^{*II}(\bar{x})$ are given by:

$$\varepsilon_{ij}^{*I}(x) = B_{ij}^I + B_{ijk}^I x_k + B_{ijkl}^I x_k x_l + \dots \quad (13)$$

$$\varepsilon_{ij}^{*II}(\bar{x}) = B_{ij}^{II} + B_{ijk}^{II} \bar{x}_k + B_{ijkl}^{II} \bar{x}_k \bar{x}_l + \dots \quad (14)$$

Additionally, the following relation holds between the coordinate system of particle I and that of particle II :

$$x_i - c_i = a_{ij} \bar{x}_j \quad (15)$$

where vector c_i and tensor a_{ij} indicate the respective relative difference between the origins of the two coordinate systems and the direction cosine of the two coordinate systems. We must solve Eqs.13 to 15 for B_{ij}^I , $B_{ijk}^I, B_{ijkl}^I, \dots, B_{ij}^{II}, B_{ijk}^{II}, B_{ijkl}^{II}, \dots$. Such a problem, however, is too complicated to solve, so we try to simplify the problem by considering the following assumptions.

- All particles are of the same material.

$$D_2^I = D_2^{II} = D_2 \quad (16)$$

- All particles have the same direction.

$$x_i - c_i = \bar{x}_i \quad (17)$$

- All particles have the same shape and size.

$$\varepsilon^{*I}(x) = \varepsilon^{*II}(\bar{x}) = \varepsilon^*(x) \quad (18)$$

- The eigenstrain is uniform in a particle.

$$\varepsilon^*(x) = \varepsilon^* \quad (19)$$

Under these assumptions, the double-particle model in Fig. 2 reduces to the simplified model seen in Fig. 3. The equivalent equation for the double-particle model is then represented by applying Eqs.16 to 19 to Eqs. 11 and 12, as follows:

$$D_2 : (\varepsilon_0 + \varepsilon_2^c) = D_1 : (\varepsilon_0 + \varepsilon_2^c - \varepsilon^*) \quad \text{in } \Omega^I, \Omega^{II} \quad (20)$$

This formula is the same as Eq. 4 in the single-particle model. The eigenstrain is solved essentially as it was in the single-particle model. However, both particles I and II influence ε_1^c and ε_2^c . According to Mura's reference [Moschovidis and Mura (1975)], ε_1^c and ε_2^c are given as follows:

$$\varepsilon_1^c = \varepsilon_1^{cI} + \varepsilon_1^{cII} = (S_{out}^I(x) + S_{out}^{II}(\bar{x})) : \varepsilon^* \quad (21)$$

$$\varepsilon_2^c = \varepsilon_2^{cI} + \varepsilon_2^{cII} = (S_{in}^I + S_{out}^{II}(\bar{x})) : \varepsilon^* \quad (22)$$

In the double-particle model, ε_1^c and ε_2^c are represented by the product of the sum of the Eshelby's tensors pertaining to each particle and the eigenstrain. Under the assumptions of Eqs.16 to 19, we can extend Eqs.21 and 22 to a general multi-particle model in which more than two particles are included by replacing the sum of the Eshelby's tensors in those equations with more than two terms. In consideration of particle interaction, Eqs.5 to 8 are modified as follows for a general multi-particle model:

$$\varepsilon^* = A_0 : \varepsilon_0 \quad (23)$$

$$A_0 = [(I \otimes I - (D_1^e)^{-1} : D_2^e)^{-1} - S_{sum2}]^{-1} \quad (24)$$

$$\varepsilon_1(x) = [I \otimes I + S_{sum1}(x) : A_0] : \varepsilon_0 \quad (25)$$

$$\varepsilon_2 = [I \otimes I + S_{sum2} : A_0] : \varepsilon_0 \quad (26)$$

$$\sigma_1(x) = D_1^e : [I \otimes I + S_{sum1}(x) : A_0] : \varepsilon_0 \quad (27)$$

$$\sigma_2 = D_2^e : [I \otimes I + S_{sum2} : A_0] : \varepsilon_0 \quad (28)$$

$$S_{sum1}(x) = S_{out}^I(x) + S_{out}^{II}(\bar{x}) + \dots \quad (29)$$

$$S_{sum2} = S_{in}^I + S_{out}^{II}(\bar{x}) + \dots \quad (30)$$

where $S_{sum1}(x)$ and S_{sum2} indicate the respective influence of each particle on the matrix material

and on the particle Ω^I . Using these equations, we can analytically calculate the strain and stress at an arbitrary point in the multi-particle model as well as in the single-particle model. We can then obtain the distributions of strain and stress in the matrix from the results. The number of terms in $S_{sum1}(x)$ and S_{sum2} increases with an increase in the number of particles. Even with a large number of particles, the strain and stress remain finite because the influence of particles far from the point of interest is small enough to be neglected.

3 Macroscopic constitutive equation

In this section, we derive a macroscopic constitutive equation for the multi-particle model from the equations shown in the previous section. Fig. 4 depicts a unit cell in the present model, consisting of numerous background cells for numerical integration, which will be mentioned later. For the unit cell, we define the average strain of the matrix $\bar{\epsilon}_1$ and that of the inclusion $\bar{\epsilon}_2$ as follows:

$$\bar{\epsilon}_1 = \frac{1}{V_1} \int_{V_1} \epsilon_1 dV, \quad \bar{\epsilon}_2 = \frac{1}{V_2} \int_{V_2} \epsilon_2 dV \quad (31)$$

where V_1 , V_2 and V are the respective volume of the matrix, that of the inclusion, and the overall volume. We assume that the average strain of the overall volume $\bar{\epsilon}$ is given as:

$$\bar{\epsilon} = (1 - f)\bar{\epsilon}_1 + f\bar{\epsilon}_2, \quad (32)$$

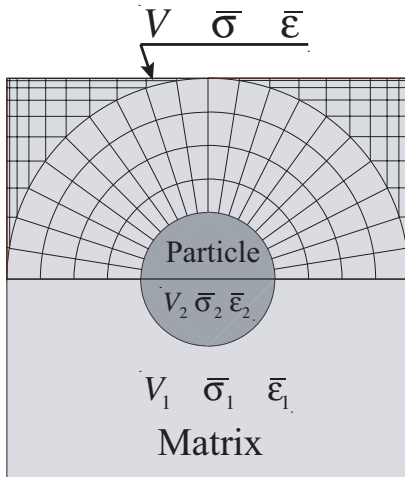


Figure 4: A unit cell in the present model

where f is the particle volume fraction. By substituting Eqs.7, 8 and 31 into Eq. 32, $\bar{\epsilon}$ is written as a function of ϵ_0 as follows:

$$\bar{\epsilon} = \alpha : \epsilon_0, \quad (33)$$

$$\alpha = \frac{1}{V} \left[\int_{V_1} I \otimes I + S_{sum1}(x) : A_0 dV + \int_{V_2} I \otimes I + S_{sum2} : A_0 dV \right] \quad (34)$$

Similarly, the average stress in the matrix $\bar{\sigma}_1$, that in the inclusion $\bar{\sigma}_2$ and that of the overall volume $\bar{\sigma}$ are written as:

$$\bar{\sigma}_1 = \frac{1}{V_1} \int_{V_1} \sigma_1 dV, \quad \bar{\sigma}_2 = \frac{1}{V_2} \int_{V_2} \sigma_2 dV, \quad (35)$$

$$\bar{\sigma} = \beta : \epsilon_0, \quad (36)$$

$$\beta = \frac{1}{V} \left[\int_{V_1} D_1^e (I \otimes I + S_{sum1}(x) : A_0) dV + \int_{V_2} D_2^e (I \otimes I + S_{sum2} : A_0) dV \right], \quad (37)$$

The average stress $\bar{\sigma}$ is written as a function of ϵ_0 as well as the average strain $\bar{\epsilon}$. α and β are the fourth-order tensors that relate the average strain and the average stress to the strain at the infinite location. Finally, we obtain the relationship between the average stress and the average strain by eliminating ϵ_0 from Eqs. 33 and 36 as follows:

$$\bar{\sigma} = \bar{D}^e : \bar{\epsilon} = \beta : \alpha^{-1} : \bar{\epsilon} \quad (38)$$

We can regard the above as a constitutive equation for a particle-dispersed composite material. When the matrix material is in a plastic state and the inclusion remains elastic, a constitutive equation for the elastic-plastic problem can be obtained by changing the elastic matrix of the matrix material D_1^e in Eqs.24 and 37 to the elastic-plastic matrix of the matrix material D_1^{ep} and revising Eq. 38 to an incremental form. The constitutive equation for the elastic-plastic problem in a particle-dispersed

composite material is given as follows:

$$d\bar{\sigma} = \bar{D}^{ep} : d\bar{\epsilon} = \beta : \alpha^{-1} : d\bar{\epsilon}, \quad (39)$$

$$\alpha = \frac{1}{V} \left[\int_{V_1} I \otimes I + S_{sum1}(x) : A_0 dV + \int_{V_2} I \otimes I + S_{sum2} : A_0 dV \right], \quad (40)$$

$$\beta = \frac{1}{V} \left[\int_{V_1} D_1^{ep} (I \otimes I + S_{sum1}(x) : A_0) dV + \int_{V_2} D_2^e (I \otimes I + S_{sum2} : A_0) dV \right], \quad (41)$$

where

$$A_0 = \left[\left(I \otimes I - \left(\bar{D}_1^{ep} \right)^{-1} : D_2^e \right)^{-1} - S_{sum2} \right]^{-1} \quad (42)$$

Numerical integration is required to calculate α and β for either an elastic problem or an elastic-plastic problem. Fig. 4 indicates the background cells used for the numerical integration. Due to symmetry, the numerical integration is performed over only a half-region. When the matrix material is in a plastic state and the inclusion remains elastic, the incremental strain and stress in the matrix material are given by the following equation, derived by replacing D_1^e with D_1^{ep} in Eqs.25 and 27:

$$d\epsilon_1(x) = (I \otimes I + S_{sum1}(x) : A_0) : d\epsilon_0, \quad (43)$$

$$d\sigma_1(x) = D_1^{ep} : (I \otimes I + S_{sum1}(x) : A_0) : d\epsilon_0. \quad (44)$$

Fig. 5 presents a flow chart of the present calculation scheme. First, the strain increment is calculated at each integral point of the finite elements in the macroscopic domain. In the microscopic domain, this strain increment is expressed as the average strain increment. The strain increment and the stress increment at each point in the matrix material are calculated in the microscopic domain. The macroscopic elastic-plastic matrix is obtained after the integral loop for the microscopic domain. In the macroscopic domain, this matrix is given at each integral point of the finite elements and is utilized as a homogenized elastic-plastic matrix in a conventional FE analysis.

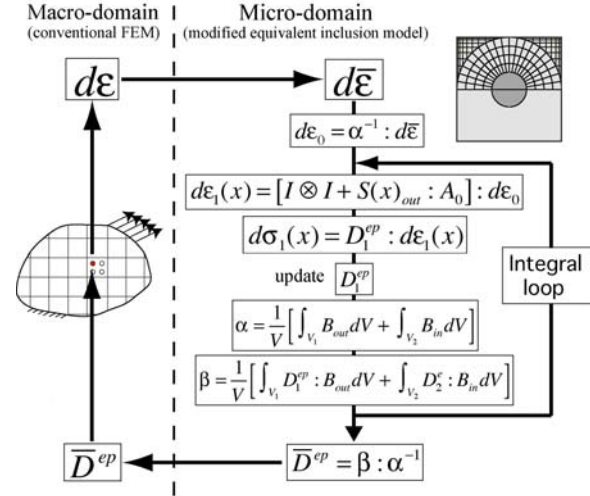


Figure 5: Flow chart of the present method

4 Gradient plasticity

According to gradient plasticity [Aifantis (2001)], the equivalent stress $\bar{\sigma}$ is defined by :

$$\bar{\sigma} = \kappa(\bar{\epsilon}) - c\nabla^2\bar{\epsilon} \quad (45)$$

where $\bar{\sigma}$, $\bar{\epsilon}$, $\kappa(\bar{\epsilon})$ and c denote the respective equivalent stress, the equivalent plastic strain, a conventional homogeneous part of flow stress, and a phenomenological gradient coefficient. $\nabla^2\bar{\epsilon}$ is a strain gradient term that permits the inclusion of a length scale in the plastic constitutive equation. Next, we define a yield function as $F = \bar{\sigma} - \kappa(\bar{\epsilon}) + c\nabla^2\bar{\epsilon}$. Using this yield function, we obtain a modified Prandtl-Reuss equation including a strain gradient term as follows:

$$d\sigma = D^{ep} d\epsilon, \quad (46)$$

$$D^{ep} = D^e - \frac{d_D d_D^T}{\left(1 - \frac{c\nabla^2\epsilon^p}{\sigma_y}\right) \left(H' - c \frac{d\nabla^2\epsilon^p}{d\epsilon^p}\right) + d_D^T a}, \quad (47)$$

$$a^T = \left[\frac{\partial F}{\partial \sigma_x}, \frac{\partial F}{\partial \sigma_y}, \frac{\partial F}{\partial \sigma_z}, \frac{\partial F}{\partial \tau_{yz}}, \frac{\partial F}{\partial \tau_{zx}}, \frac{\partial F}{\partial \tau_{xy}} \right] \quad (48)$$

where D^{ep} denotes the elastic-plastic matrix, D^e is the elastic matrix, H' is the rate of strain hardening, and $d_D = D^e a$. If the gradient coefficient c is zero, Eq. 47 is the same as the conventional Prandtl-Reuss equation. We utilize Eq. 45 and

Eqs. 46 and 47 as the yield criterion and elastic-plastic constitutive equations in the present analysis. Eq. 47 is used for D^{ep} in the flow chart in Fig. 5.

5 Numerical example

5.1 Analysis conditions

We performed a homogenized finite element analysis using the elastic-plastic constitutive equation based on the modified version of the Eshelby's equivalent inclusion method combined with gradient plasticity. In this analysis, we consider two domains, a macroscopic domain and a microscopic domain. Fig. 6 illustrates the concept of this analysis. We assume that the particles have a circular shape and that all have the same diameter. We apply the conventional finite element method to the macroscopic domain with a homogeneous material subjected to uniaxial tensile loading. For the macroscopic analysis, we employ the macroscopic elastic-plastic constitutive equation in Eqs. 39 to 42, in which D^{ep} given by Eq. 47 is used to take the gradient plasticity into account. In the microscopic domain, we obtain the strain and stress distributions around a particle using the strain calculated from the macroscopic analysis. We calculate the strain gradient term by differentiating a polynomial expression

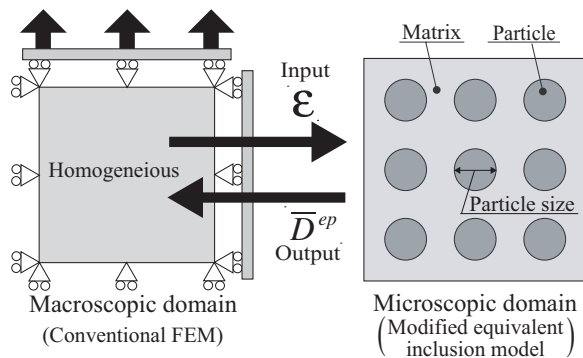


Figure 6: Numerical model

Table 1: Material parameters

	E [GPa]	σ_y [MPa]	ν	B [MPa]	n
Matrix	76.0	205.0	0.33	280.0	30
Particle	410.0	-	0.33	-	-

of the strain distribution obtained using the least square method. The material properties used in the present study are summarized in Tab. 1, where E, σ_y and ν denote the respective Young's modulus, the yield stress and the Poisson's ratio and B and n are the coefficients of the Ramberg-Osgood relation given by

$$\varepsilon = (\sigma/E) + (\sigma/B)^n \quad (49)$$

These material properties correspond to those of Al-SiC composite materials, in which SiC particles are dispersed in an Al matrix [Lloyd (1994)]. In addition, we need to determine the gradient coefficient c in Eq. 45. This coefficient should be measured experimentally [Aifantis (2000)]. One way of measuring it is to use initial yield data for specimens of varying grain size for polycrystalline materials and varying particle size for particle-dispersed composite materials. We are unable to find such data, thus, in the present study we choose the gradient coefficient c as zero in the case where the strain gradient effect is not considered and -0.01 N in the case where the strain gradient effect is considered.

5.2 Results and discussion

The results for the strain distribution around a particle and the stress-strain relation at the loading location without the strain gradient effect ($c = 0$) are presented in Figs.7 and 8. The results are in good agreement with conventional FEM results. We confirmed that the present model, using the modified equivalent inclusion model, has sufficient accuracy.

The stress-strain relation at the loading location is presented in Fig. 9 for a particle volume fraction f of 15%. We utilized five particle sizes, $32\mu m$, $16\mu m$, $12\mu m$, $9\mu m$, and $7\mu m$ when investigating the size effect. Fig. 10 (a) shows the variation in the 0.2% offset yield stress with particle size. When the particle is large, the stress-strain curves become almost independent of particle size. As the particle becomes smaller, the yield stress and the tangent modulus in the plastic range become larger. Experiment results [Aikin and Christodoulou (1991)] are given in Fig. 10 (b). Although the particle material used in their

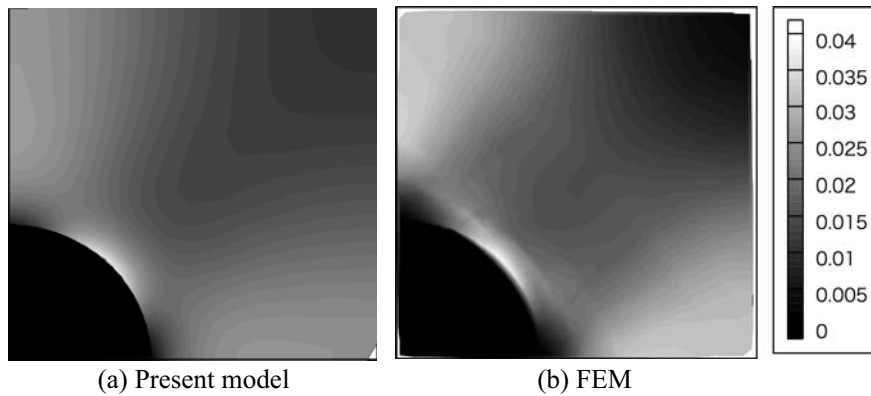


Figure 7: Strain distribution without the strain gradient effect ($c = 0$) when the macroscopic strain is 0.015 (a) Present model (b) conventional FEM.

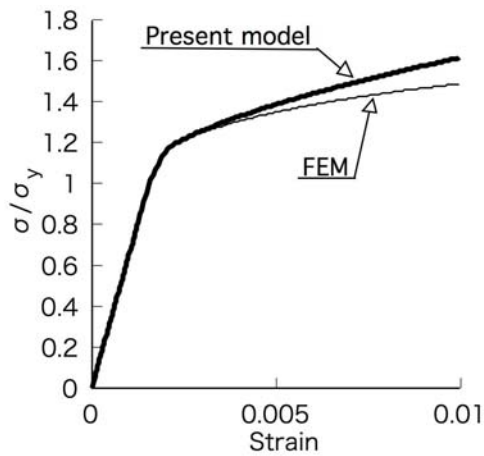


Figure 8: Macroscopic stress-strain relation without the strain gradient effect ($c = 0$)

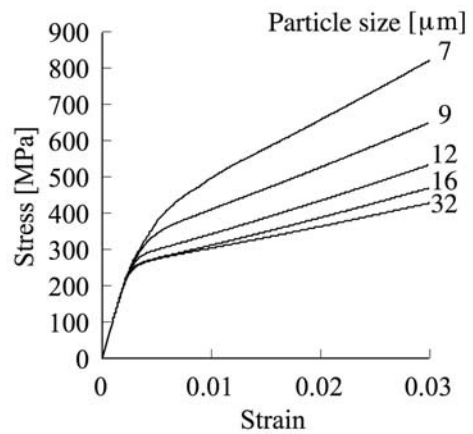


Figure 9: Stress-strain curve depending on particle size ($c = -0.01$)

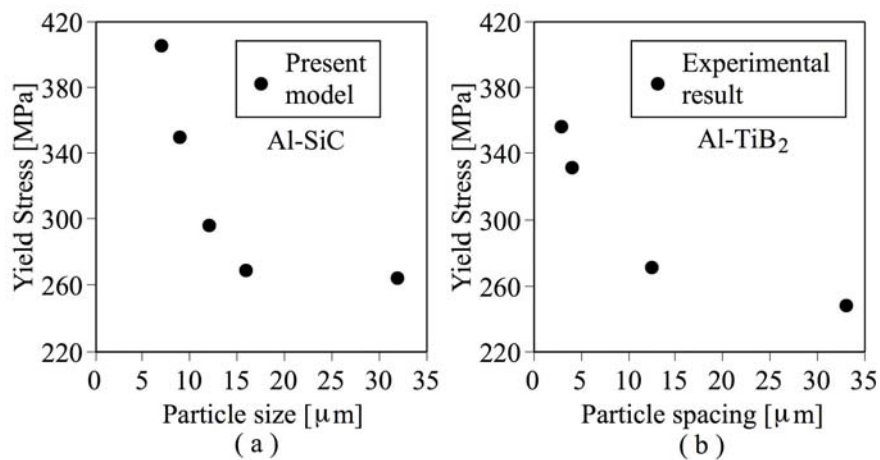


Figure 10: 0.2 % offset yield stress. (a) Results of the present study (b) Experimental results

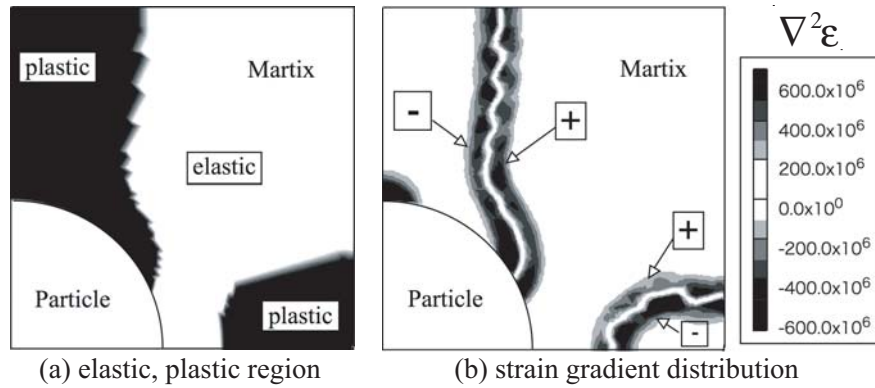


Figure 11: Plasticity and strain distribution domain when the macroscopic strain is 0.002 and coefficient c is zero.

experiment differs from the present study, the results of the present calculation are similar to the experiment results. The analytical results agree with the experiment results, demonstrating that a particle-dispersed composite material with a smaller particle has greater mechanical strength [Lloyd (1994), Zhu, Zbib, and Aifantis (1997), Ling (2000)]. Fig. 11 depicts the strain gradient distribution when the macroscopic strain is 0.002 and coefficient c is zero. The strain gradient distribution exhibits positive values at the outer peripheral region around the plastic domain. If coefficient c is positive, the yield stress near the outer boundary around the plastic regions decreases, according to Eq. 45. In this case, plastic deformation will be promoted. In contrast, if coefficient c is negative, the yield stress near the outer boundary around the plastic regions increases. In this case, plastic deformation will be suppressed. The present study corresponds to the latter case.

6 Summary

In the present study, we derived a macroscopic elastic-plastic constitutive equation for a particle-dispersed composite material based on the Eshelby's equivalent inclusion method and gradient plasticity. We incorporated this macroscopic elastic-plastic constitutive equation into a finite element program and performed a homogenized finite element analysis of a particle-dispersed composite material, by which both the macroscopic and microscopic behaviors of the composite material were obtained. The present

method is able to conclusively demonstrate the effect of particle size on the strength of a composite material. Very efficient computation can be performed for structures composed of composite materials using the present method, since it uses the homogenized elastic-plastic constitutive equation derived from the modified equivalent inclusion model in the finite element analysis and does not need a fine-element mesh to represent the dispersed particles.

References

- Aifantis, E. C.** (2000): theoretical and experimental aspects of gradient theory. *SEM IX International Con. Exp. Mech.*, pp. 648–651.
- Aifantis, E. C.** (2001): Gradient Plasticity. In *Handbook of Materials Behavior Models*, chapter 4.12. Academic Press, New York.
- Aikin, Jr., R. M.; Christodoulou, L.** (1991): The role of equiaxed particles on the yield stress of composites. *Scripta METALLURGICA et MATERIALIA*, vol. 25, no. 15, pp. 9–14.
- Eshelby, J. D.** (1957): The determination of the elastic field of an ellipsoidal inclusion, and related problems. *Proc. of the Royal Society of London Series A - Mathematical and Physical Sciences*, vol. 241A, no. 1226, pp. 376–396.
- Ling, Z.** (2000): Deformation Behavior and Microstructure Effect in 2124Al/AiC_p Composite. *Journal of COMPOSITE MATERIALS*, vol. 02, no. 34, pp. 101–115.

Liu, X.; Hu, G. (2005): A continuum micromechanical theory of overall plasticity for particulate composites including particle size effect. *International Journal of Plasticity*, vol. 21, pp. 777–799.

Lloyd, D. J. (1994): Particle reinforced aluminium and magnesium matrix composite. *International Material Reviews*, vol. 39, no. 1, pp. 1–23.

Mori, T.; Tanaka, K. (1973): Average stress in matrix and average elastic energy of materials with misfitting inclusions. *ACTA METALLURGICA*, vol. 21, pp. 571–574.

Moschovidis, Z. A.; Mura, T. (1975): Two-Ellipsoidal Inhomogeneities by the Equivalent Inclusion Method. *Journal of Applied Mechanics*, pp. 847–852.

Nakagaki, M.; Takashima, S.; Matsumoto, R.; Miyazaki, N. (2005): An Aspect of Hall-Petch Effect in Metallograin Structure. *CMES: Computer Modeling in Engineering & Sciences*, vol. 10, no. 3, pp. 199–208.

Needleman, A. (2000): Computational Mechanics at The Mesoscale. *Acta Materialia*, vol. 48, pp. 105–124.

Tandon, G. P.; Weng, G. J. (1988): A Theory of Particle-Reinforced Plasticity. *Journal of Applied Mechanics*, vol. 55, pp. 126–135.

Yefimov, S.; Groma, I.; Giessen, E. (2004): A comparison of a statistical-mechanics based plasticity model with discrete dislocation plasticity calculations. *Journal of the Mechanics and Physics of Solids*, vol. 52, pp. 279–300.

Zhu, H. T.; Zbib, H. M.; Aifantis, E. C. (1997): Strain gradients and continuum modeling of size effect in metal matrix. *Acta Mechanica*, vol. 121, pp. 165–176.